ISSN 1560-0904, Polymer Science, Series B, 2023, Vol. 65, No. 2, pp. 160–169. © Pleiades Publishing, Ltd., 2023.
ISSN 1560-0904, Polymer Science, Series B, 2023. © Pleiades Publishing, Ltd., 2023.

COMPOSITES

Preparation and Characterization of Graphene Oxide/Waterborne Polyurethane Composites

Li Guoqian[a,b], Xu Jianwei[a], Guan Aizhang[c], Xiaomin Li[b], Yang Kainuo[b], Shibo Qiu[a,b,*], Linhong Liu[a,b], Li Houbin[a], and Liu Xinghai[a,]**

[a] *Research Center of Graphic Communication, Printing and Packaging, Wuhan University, Hubei Province, China*
[b] *Wuhan Danyaxiang Biological Technology Co. Ltd., Wuhan, 430040 China*
[c] *China Tobacco Hubei Industrial LLC, Wuhan, 430040 China*
**e-mail: qiushb@hjl.hbtobacco.cn*
***e-mail: liuxh@whu.edu.cn*

Received September 5, 2022; revised December 28, 2022; accepted December 30, 2022

Abstract—A composite material with excellent thermal, mechanical and optical properties was prepared by compounding modified graphene oxide with aqueous polyurethane. Graphene oxide was prepared from graphite and modified with a silane coupling agent, 3-aminopropyltriethoxysilane. Composite emulsions were prepared by reacting of modified graphene oxide containing an amino group with the isocyanate group of polyurethane prepolymer. The successful synthesis was confirmed by IR spectroscopy and XRD tests. Comparing the mechanical and thermal properties of physically blended graphene oxide and polyurethane, polyurethane and modified graphene oxide with polyurethane has revealed that the tensile strength and the thermal stability of the latter was significantly improved.

DOI: 10.1134/S1560090423700811

INTRODUCTION

Graphene, a single atomic layer of graphite, is currently considered to be one of the materials with disruptive technologies and has been attracting widespread attention from academia and industry. Since the first successful preparation of graphene by Andre Geim and Konstantin Novoselov, graphene has continued to spark innovation in various technological fields, such as quantum computing [1], smart sensing, flexible electronics, and medical devices [2]. Other derivatives of graphene, such as graphene oxide (GO), reduced graphene oxide (rGO), multilayer graphene (FLG) and graphene nanoparticles (GNPs) are widely used in polymer composites.

The properties of waterborne polyurethanes (WPU) can be improved by adding reinforcement to the polymer matrix, enhancing thermal, electrical, mechanical, and biological properties. In recent years, there have been an increasing number of reports on polyurethane/graphene composites [3]. In terms of mechanical properties, studies have shown that the incorporation of graphene and its derivatives typically increases the Young's modulus of WPU, and the extent of this enhancement depends on the level of graphene dispersion and the matrix structure and properties of WPU. However, the increase in modulus of elasticity may be accompanied by a decrease in the tensile strength or elongation at the break of the WPU due to weakening of the polymer chain-to-chain interaction. Extensive research has now demonstrated that the addition of graphene into the WPU can decrease the tensile strength and elasticity modulus and increase the elongation at break, i.e. the flexibility and extensibility of these composites improved. For example, Kim et al. found a 623% increase in elastic modulus and a 105.4 and 43.16% decrease in elongation at break and tensile strength, respectively, for GO/WPU composites added at 1 wt % [4]. Ting Wan et al. found that the tensile strength of nanocomposites incorporating 0.5 wt % GO/WPU was 22–47% higher than that of pure aqueous polyurethane [5].

In terms of thermal properties, the introduction of graphene into WPU has been shown to improve significantly its thermal stability and thermal conductivity. Zhu et al. found that the thermal stability of the composites was significantly better when GO was added to WPU, and the glass transition temperature of the composites was enhanced from –72 to –68°C [6]. A study by Kale et al. showed that with 0.2 wt % of GO/SiO_2, the decomposition temperature of the WPU increased by approx. 44%. Although the performance of graphene materials in improving, the thermal stability of WPU is remarkable, the reason for this phenomenon is not clear [7]. Meanwhile, Lei et al. introduced (3-(2-aminoethyl) aminopropyl) trimethoxysilane (AEAPTMS) as a chain extender during

the synthesis of WPU and prepared organosilicon modified WPU, which improved heat resistance, tensile strength and adhesion strength of WPU on nonpolar oriented polypropylene films [8]. Experiments showed that when the mass fraction of AEAPTMS increased gradually from 0 to 5 wt %, the glass transition temperature of WPU increased from −54 to −51°C; the decomposition temperature of 5% weight loss increased by 16°C, the thermal stability was substantially improved, while the tensile strength of the WPU adhesive film increased by 95%. Cheng Xiang used a silane coupling agent (γ-glycidyl ether oxypropyl trimethoxysilane, KH560) to undergo a condensation reaction with WPU containing carboxyl groups, followed by a hydrolytic condensation reaction with an organosilicon compound (ethyl orthosilicate, TEOS) to form a reticular structure, and successfully prepared a silica-modified hydroxyl type WPU with stable properties [9]. Experiments showed that the initial decomposition temperature of the WPU material increased from 254 to 271°C, which enhanced the thermal stability of the WPU coating.

In this study, GO was prepared by the Hummers method [10], and modified GO (f-GO) containing amino groups was prepared using APTES. Finally, the f-GO was covalently bonded to the WPU matrix using APTES as a "bridge", resulting in a composite material with excellent thermal and mechanical properties that can be used as a ligand for aqueous inks.

EXPERIMENTAL

Materials

1,4-Butanediol, triethylamine, acetone, potassium permanganate, dibutylamine, toluene, sodium hydroxide, hydrochloric acid, concentrated sulphuric acid, hydrogen peroxide and ammonia were purchased from Sinopharm Co. Chemical Reagent Co. Nitrogen gas was purchased from Wuhan Xiangyun Industry and Trade Co. Water-based polyurethane was purchased from Shenzhen Ji Tian Chemical Co. All the chemicals used in this work were not purified further.

Preparation of f-GO/WPU Composites

The GO powder was prepared from graphite powder using Hummers' method. Aiming this, 23 mL of concentrated H_2SO_4 was chilled to 0°C, and 0.5 g of graphite powder and 0.5 g of $NaNO_3$ were added to the concentrated H_2SO_4 and mechanically stirred until homogeneous. Then, 3 g of $KMnO_4$ was slowly added upon stirring and the temperature was kept below 5°C. The temperature was increased to 35°C and the mixture was stirred for 2 h until a paste was formed. After that, 40 mL of deionized water was added slowly and the temperature was kept below 50°C. Then the temperature was increased to 95°C for 0.5 h. Deionized water (100 mL) was added and 20 mL of H_2O_2 (30 wt %) was poured in several portions with stirring to obtain a golden yellow solution. The solution was centrifuged and washed with 180 mL of HCl at a concentration of 10 wt %, and then with 180 mL of H_2O. Finally, the paste is spread evenly and dried in an oven for 12 h.

The 100 mg of GO was weighed into a 250 mL round bottom flask and 100 mL of anhydrous ethanol was added to obtain a heterogeneous yellow-brown dispersion. The dispersion was sonicated for 1 h using an ultrasonic bath cleaner until it became clear and free of visible particulate matter. Then 100 mg of GO and 50 mg of *N*,*N*-dicyclohexylcarbodiimide (DCC) were dispersed in 50 mL of a mixture of APTES (3-aminopropyltriethoxysilane) and ethanol. Then 1 mL of ammonia (25 wt %) was added, sonicated for 1 h and the stirred mixture was heated in an oil bath at 30°C for 24 h [11, 12]. The graphene functionalized with APTES was washed with anhydrous ethanol and deionized water, centrifuged 5–6 times at 8000 rpm for 6 min. The resulting precipitate was dried under vacuum for 24 h to obtain f-GO powder and stored. The preparation process is shown in Scheme 1.

The 5.00 g of PTMG was weighed in 1000 in a round-bottom flask with magnetic stirring and water was removed at reduced pressure and 105°C for 2.5 h. Then 3.89 g of IPDI was added dropwise by syringe under nitrogen atmosphere at 90°C for 1 h and 1.01 g of DMPA was added and reacted for 3 h. The reaction was carried out at 90°C for 3 h. If the viscosity of the reactant increased, an appropriate amount of anhydrous acetone was added dropwise to reduce the viscosity. The 0.45 g of BDO was added to expand the chain, and 1 drop of dibutyltin dilaurate catalyst was added and reacted at 90°C for 3 h. The reaction was cooled down to 35°C and the solvent was removed with a rotary evaporator for about 35 min to obtain the WPU prepolymer. Then 100 mg of f-GO powder was dispersed in 100 mL of acetone and sonicated for 1 h. The 19.9 g of polyurethane prepolymer, 0.76 g of TEA and 10.95 g of deionized water were added to the above f-GO suspension and dispersed at high speed (1300 r/min) in a flask at room temperature for 35 min. Then the solvent was removed to obtain the f-GO/WPU composite emulsion. The preparation process is shown in Scheme 2.

Finally, the f-GO/WPU composite emulsion was poured into a PTFE mold and dried at room temperature for 48 h. The composite films were obtained after peeling.

GO/WPU films are then prepared. The 100 mg of GO was homogeneously dispersed in 19.90 g of solid WPU emulsion for 12 h after being sonicated for 2 h. This results in a GO/WPU film-forming solution with a mass fraction of 0.5%. The film-forming solution was poured into a PTFE mold and dried at 25°C for

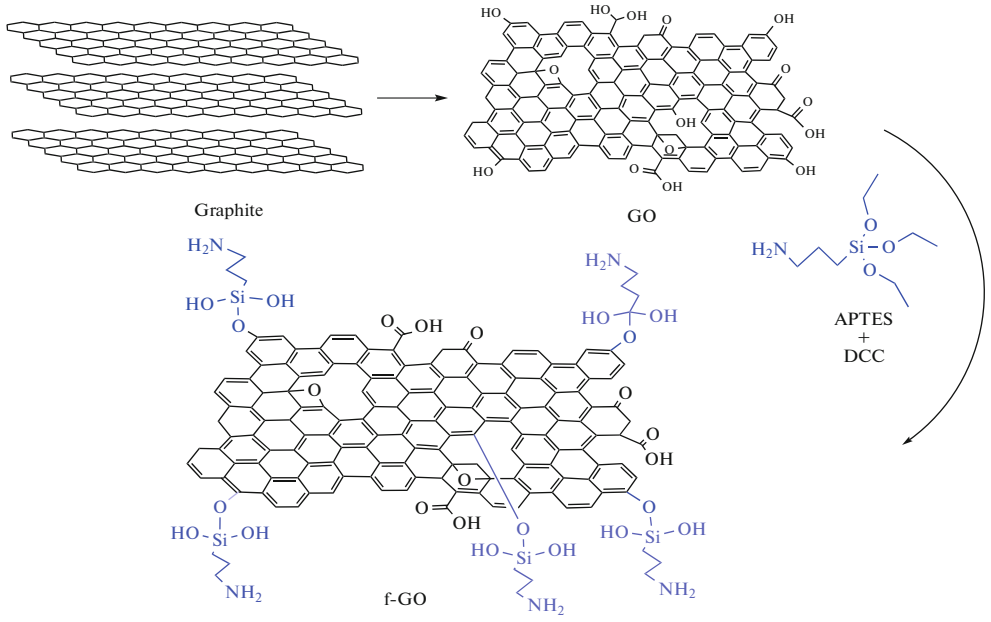

Scheme 1.

48 h. The GO/WPU physical hybrid film was obtained after peeling.

Finally, the pure WPU film is prepared. Pour the commercial pure WPU emulsion into the mold and dry at room temperature for 48 h to obtain WPU film.

Testing and Analysis Methods

The samples were tested using a NICOLET IS50 infrared spectrometer (Therno Fisher Scientific Co., USA). Potassium bromide powder was dried at 130°C for 24 h until free of residual solvent. GO and f-GO were mixed well with potassium bromide at a mass ratio of 100 : 1 and then thoroughly ground in dry mortar (particles of about 2 μm) and baked under a high heat lamp to ensure that no moisture remained. Thin slices of transparent samples were pressed on a tablet press with a scanning range of 4000–400 cm^{-1}.

XRD tests were carried out on film and powder samples using an X-ray diffractometer (Rigaku Mini-Flex 600, Rigaku Corporation, Japan). The powders were placed in a vacuum drying oven for 18 h to dry out moisture and impurities, ground and then laid flat in the grooves of the sample sheet. The thin film samples were cut into 2.5 × 2.5 cm squares and placed on the reflective sample sheet for testing. The scanning angle range was 5°–80°.

The surface morphology of the film and powder samples was measured using a field emission scanning electron microscope (Zeiss SIGMA FESEM, Zeiss AG, Germany). The powder sample was dissolved in anhydrous ethanol, sonicated for 2 h and dropped onto the silicon wafer to dry naturally. The thin films were cut into small pieces and pasted onto conductive adhesive to test the surface profile. The thin films were cold quenched in liquid nitrogen to obtain smooth sections and pasted vertically onto the cylindrical surface of copper wafers to test the section profile. The test samples were sprayed with gold for 30 s at an accelerating voltage of 5.0 kV.

The mechanical properties of the film samples were tested using a 3340 series tensile testing machine (Ingstrom (Shanghai) Laboratory Equipment Trading Co.), where the Young's modulus, tensile strength and elongation at break were calculated using the formulae of GB/T 228.1–2021 "Metal Materials Tensile test Part 1: Room temperature test method". The film samples were cut into a dumbbell shape, where the length L of the test section was 25 mm, the width b was 5 mm, the thickness d was 1 mm and the stretching rate was 10 mm/min. The results obtained are the average of 3 tests. The ambient relative humidity of this test was 40% and the temperature was 22°C.

The thermogravimetric curves of the film and powder samples were tested using an STA 2500 Regulus thermogravimetric analyzer (NETZSCH Instrument Manufacturing GmbH). Samples of 5–10 mg were weighed and placed in an alumina crucible at a temperature range of 25–600°C, with a ramp-up rate of 5 grad/min and N_2 as the protective gas.

RESULTS AND DISCUSSION

Figure 1 shows the FTIR spectra of GO and f-GO. In the FTIR spectrum of GO, the characteristic absorption band at 3425 cm^{-1} is –OH and the charac-

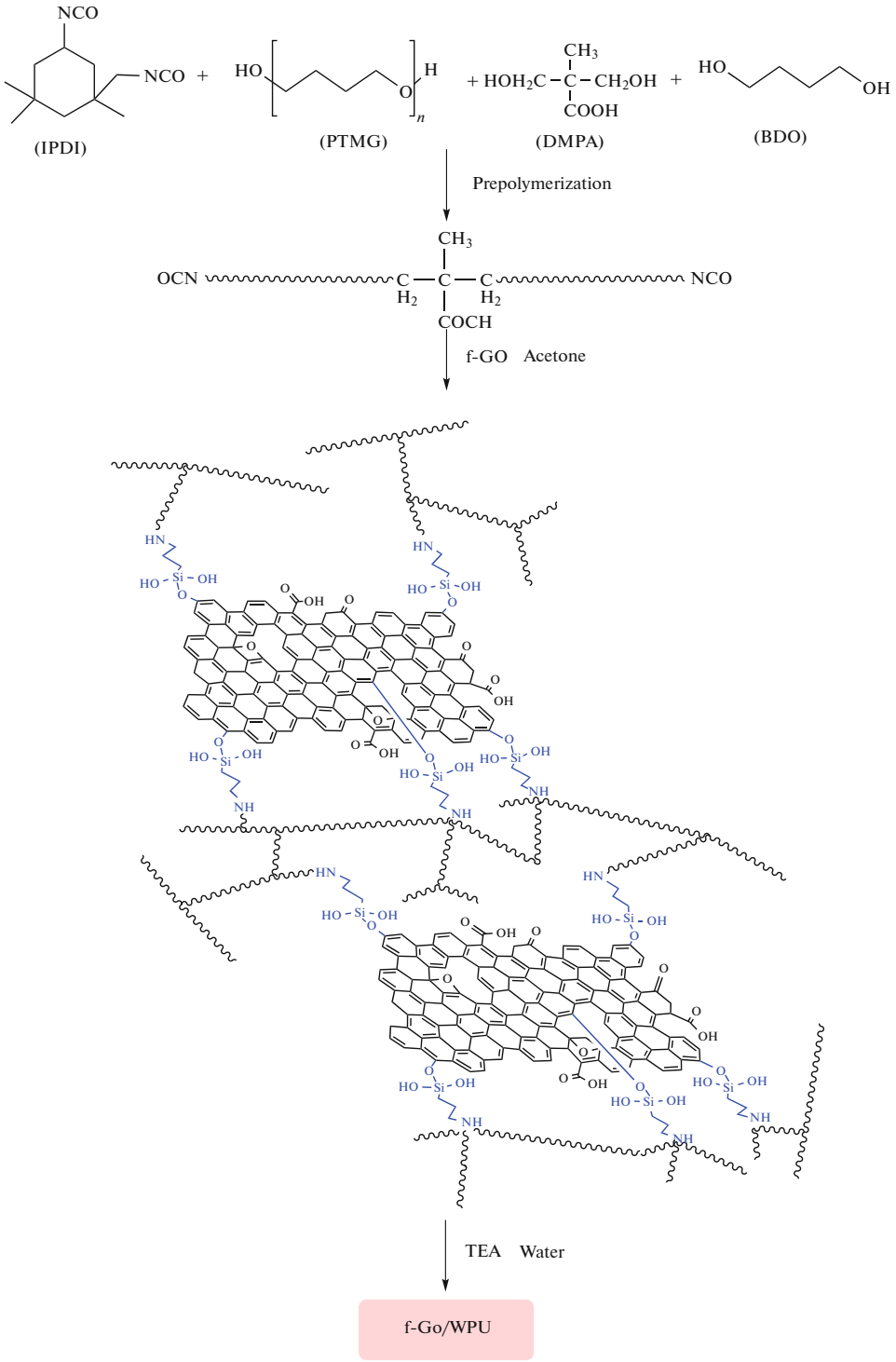

Scheme 2.

teristic absorption bands of the stretching vibrations at 1724 and 1227 cm^{-1} are C=O and –C–OH respectively. The multiple bands at about 1049 cm^{-1} correspond to C–O–C bending vibrations. These four characteristic absorption bands demonstrate the successful preparation of GO. In addition, the characteristic vibrational band of non-oxidized C=C in GO is at 1632 cm^{-1}. The in-plane deformation vibrational absorption peak of O–H is at 1402 cm^{-1}. The presence of this band is further evidence of the presence of

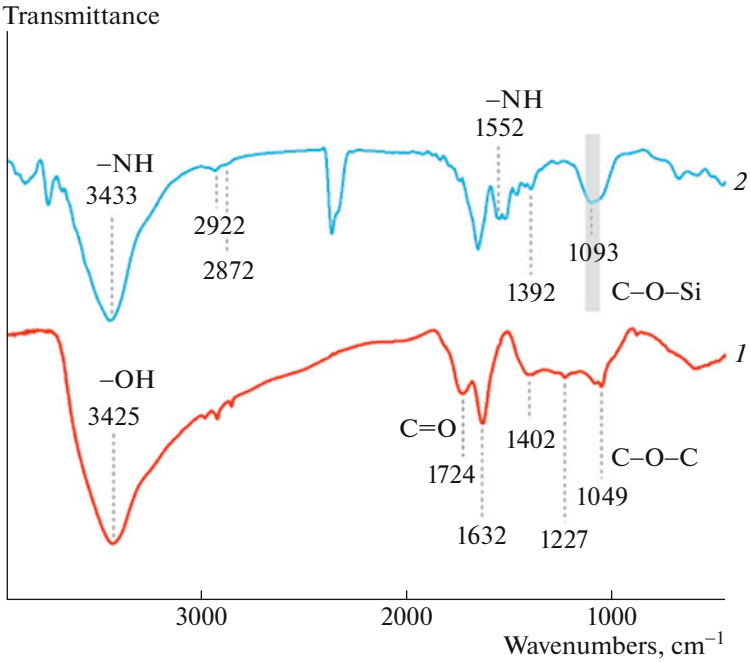

Fig. 1. Infrared spectra of (*1*) GO and (*2*) f-GO.

C–OH and the presence of hydroxyl groups makes the prepared GO hydrophilic and well dispersed in solvents such as water, acetone and ethanol.

In the FTIR spectrum of f-GO, the stretching vibrational absorption band at 3433 cm^{-1} is –NH, and the bands at 2927 and 2873 cm^{-1} are the symmetric and asymmetric characteristic vibrational bands of $-CH_2-$ in the silane-coupling agent. In comparison to GO, a distinct and intense new band, the characteristic vibrational band of –C–O–Si– appears at 1099 cm^{-1}, indicating the successful grafting of APTES to the surface of GO. In addition, the characteristic absorption band of N–H appears at 1551 cm^{-1} and the characteristic vibrational band of –C–OH at 1389 cm^{-1}, indicating the successful preparation of APTES-modified f-GO. The FTIR spectrum of f-GO shows a large signal at about 2300 cm^{-1} due to the influence of CO_2 in the environment.

Figure 2 shows the FTIR spectra of pure WPU and f-GO/WPU composites (F-GO/WPU). The two curves in the Fig. 2 show the telescopic vibrational absorption bands of N–H at 3332 and 3344 cm^{-1}, of C=O at 1716 and 1718 cm^{-1} and the bending vibrational absorption band of –CNH at 1529 cm^{-1}. The presence of these three bands proves the presence of the carbamate group, indicating the successful preparation of the WPU prepolymer. The bands at 2937 and 2861 cm^{-1} are the asymmetric stretching vibration band and the stretching vibration characteristic absorption band of C–H, respectively. Compared to the pure WPU, the f-GO/WPU composite shows a characteristic Si–C vibrational band at 802 cm^{-1}, indicating a successful composite of f-GO with WPU.

Figure 3 shows the X-ray diffraction patterns of functionalized graphene, graphene and graphite. The raw graphite before chemical exfoliation shows a strong (002) crystalline diffraction peak around $2\theta = 26.6°$, which is due to the tight regular arrangement of the crystal lamellae of graphite. After chemical exfoliation the (002) crystallographic diffraction peak near 26.6° disappears completely and shows a strong (001) crystallographic diffraction peak near $2\theta = 11.3°$, demonstrating complete oxidation of GO. The interspacing between the GO lamellae after chemical exfoliation becomes larger and is calculated by the Bragg equation to be 0.78 nm. Functionalized graphene (F-GO) shows a significantly weaker (001) crystalline diffraction peak near 11.3°, while a wider and more intense diffraction peak appears near $2\theta = 21.1°$, demonstrating a partial reduction of GO during functionalization and a reduction in the crystalline interspacing to 0.42 nm. Due to the partial removal of oxygen-containing functional groups from the GO lamellae surface during functionalization, the van der Waals forces between the f-GO lamellae are enhanced, which leads to increased agglomeration and stacking between the lamellae, resulting in a smaller interspacing between some of the f-GO lamellae. The hydroxyl groups generated by the hydrolysis of APTES undergo a condensation reaction with the oxygen-containing functional groups on the GO surface, causing them to be grafted onto the graphene surface. The larger spatial volume of the grafted APTES increases the inter-

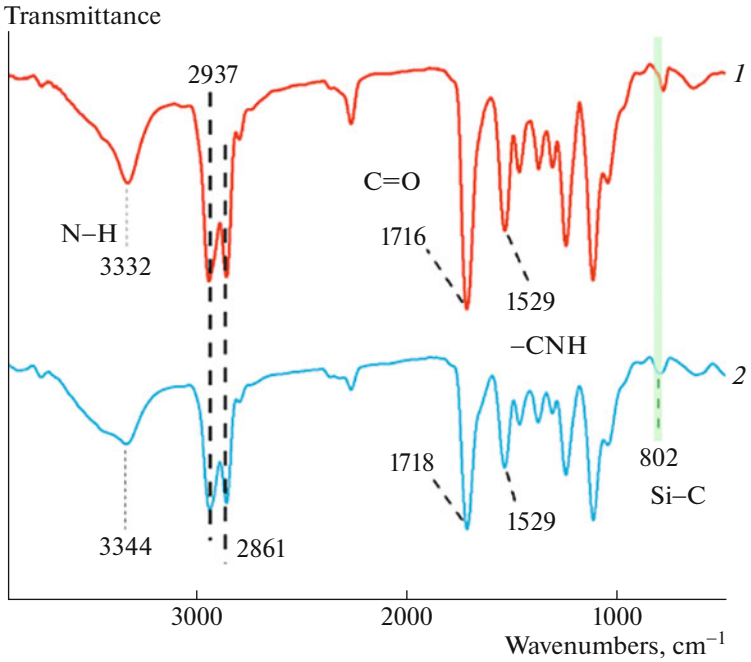

Fig. 2. Infrared spectra of (*1*) WPU and (*2*) f-GO/WPU composites.

spacing of some f-GO lamellae and results in a lower intensity spike near 2θ = 5.8°.

Figure 4 shows the XRD patterns of the graphene/WPU films prepared by chemical reaction and physical mixing. The XRD characterization results for both sides of the films (face 1 and face 2) were obtained by testing the front and back sides of the films separately for both composite methods. The XRD patterns of the chemically prepared f-GO/WPU films were similar to the results of the pure WPU films, not exhibiting the strong diffraction peak of graphene while both showing a broad diffraction peak around 19.3°, indicating the amorphous structure of the polyurethane. This proves that f-GO has been uniformly dispersed within the polyurethane film without agglomeration and therefore no diffraction peaks of f-GO can be detected on the film surface, which is consistent with the SEM characterization results. The physically blended GO/WPU film face 2 was similar to the pure WPU film, while face 1 exhibited a strong (002) crystalline diffraction peak at 2θ = 28.9°. This is due to the inability of the physically blended GO to be stable and uniform dispersed in the polyurethane emulsion. During the drying process to form the film, the GO in the composite emulsion precipitates and solidifies at the bottom of the film, resulting in a non-uniform dispersion of GO in the film, a situation that also corroborates with the SEM characterization results.

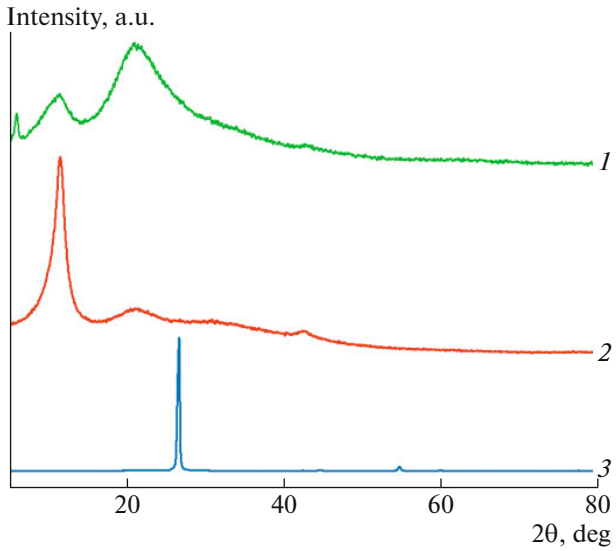

Fig. 3. X-ray diffraction patterns of (*1*) f-GO, (*2*) GO, and (*3*) graphite.

Figure 5 shows SEM images of GO, f-GO, f-GO/WPU composites and GO/WPU composites. As can be seen in Fig. 5a, the surface of prepared GO is relatively flat with some folds, indicating the existence of lamellar stacking of GO, which is due to the formation of hydrogen bonds between the oxygen-containing functional groups on the GO surface, increasing the interaction forces between the graphene lamellae [13]. As can be seen in Fig. 5b, GO modified by APTES shows thin layer overlap and agglomeration, with a significant increase in surface wrinkling, which is mainly due to the cross-linking of silicone

oxygen groups with each other after the grafting of APTES on the GO surface, resulting in poor dispersion and agglomeration. Figures 5c and 5d show the cross sections of the f-GO/WPU and GO/WPU composites by cold quenching in liquid nitrogen respectively. In Fig. 5c, it can be seen that GO is uniformly embedded inside the WPU with good dispersion, and in Fig. 5d, it can be seen that GO is mostly concentrated on the surface of the WPU film and only a small amount is dispersed inside the polyurethane. Figure 5e shows the surface morphology of the f-GO/WPU film. It can be seen that the f-GO is uniformly distributed on the WPU substrate, while in Figs. 5e, 5f the GO content of the physically mixed GO/WPU film differs significantly between the central and edge portions of the film, with GO concentrated at the edges of the film and not uniformly dispersed in the central portion of the film.

Figure 6 shows the tensile curves of the f-GO/WPU composite, GO/WPU and Pure WPU films, where the R-value (isocyanate number) of the WPU prepolymer in f-GO/WPU is 1.0. Compared to the commercial Pure WPU film, the tensile strength of the composite is increased from 8.4 to 55.8 MPa, an increase of 568%. It can be seen that f-GO can significantly improve the mechanical properties of WPU, which is mainly due to the homogeneous dispersion of f-GO matrix by APTES treatment in the WPU, the reaction of the amino group on the surface of the modified GO with the isocyanate group in the WPU prepolymer, and the dispersion of graphene in the form of covalent bonds inside the WPU, which increases the interfacial bond between f-GO and WPU and facilitates the stress and energy transfer and consumption [14], and therefore can significantly increase the tensile strength and Young's modulus of the material [15]. In terms of elongation at break, the f-GO/WPU composites decreased from 740 to 627%, mainly because the addition of f-GO restricted the movement of the WPU molecular chains, resulting in an increase in the tensile strength and a decrease in the elongation at break of the polyurethane. However, when GO was added to the WPU matrix in a physically mixed manner, the mechanical properties of the GO/WPU composites decreased, with the tensile strength decreasing from 24.0 MPa to 8.4 MPa, which proved the physical mixing of GO instead reduced the mechanical properties of the polyurethane [3]. This is mainly due to the agglomeration of GO during the film formation process and the material's own inhomogeneity which makes more stress concentration points appear during the stretching process, thus reducing the tensile strength and Young's modulus of the polymer. This can be verified by combining SEM and XRD results.

In order to investigate the mechanical properties of f-GO/WPU and GO/WPU adhesive films with different f-GO and GO contents were prepared and the differences in their mechanical properties were investigated by the methods described previously. The results are shown in Fig. 7. The tensile strength of f-GO/WPU and GO/WPU adhesive films increased with the increase of f-GO and GO content, but the elongation at break decreased with the increase of f-GO and GO content.

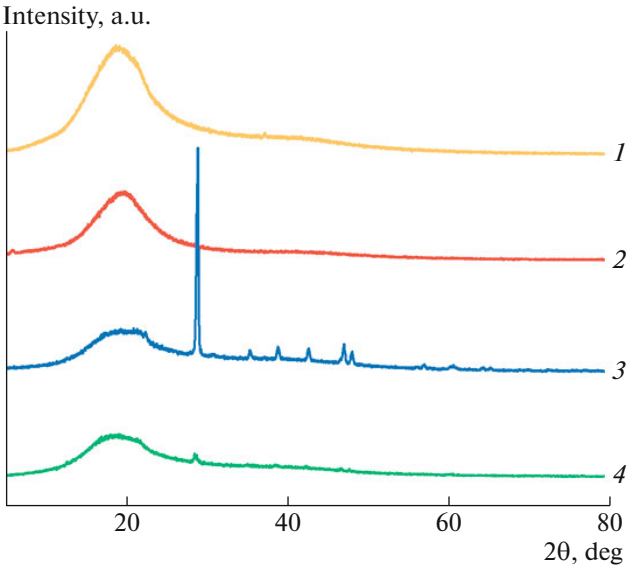

Fig. 4. XRD patterns of the f-GO/WPU films: (*1*) f-GO/WPU-face 1 and (*2*) f-GO/WPU-face 2 and GO/WPU physical hybrid films: (*3*) GO/WPU-face 1 and (*4*) GO/WPU-face 2.

Figure 8 shows the TGA curves of GO and f-GO. It can be seen that there is a significant difference in the thermal degradation properties of f-GO and GO at 600°C, with a weight loss of 49% for f-GO compared to 55% for GO. The temperature at the maximum thermal degradation rate of GO is approximately 211°C, at which point the weight loss is 32.2%. This is mainly due to the thermal decomposition of the oxygen-containing functional groups on the surface of graphene oxide [16]. Weight loss in the 211–600°C region is mainly caused by the sublimation or combustion of carbon. The temperature at the maximum thermal decomposition rate of f-GO is about 165°C with a weight loss rate of 17.6%. The temperature at which the weight loss rate is 10% (T10%) was chosen as a measure of the thermal stability of the material. T10% for GO was 61°C and for f-GO was 129°C. The overall thermal stability of f-GO was higher than that of GO, mainly due to the thermally stable siloxyl groups on the surface of the APTES-modified GO.

The aqueous dispersions of 1 mg/mL GO and f-GO after 30 min of sonication are also shown in Fig. 8. It can be observed that the aqueous solution of GO is transparent in golden color and the aqueous solution of f-GO is black in color, both uniformly dispersed in water with good dispersibility.

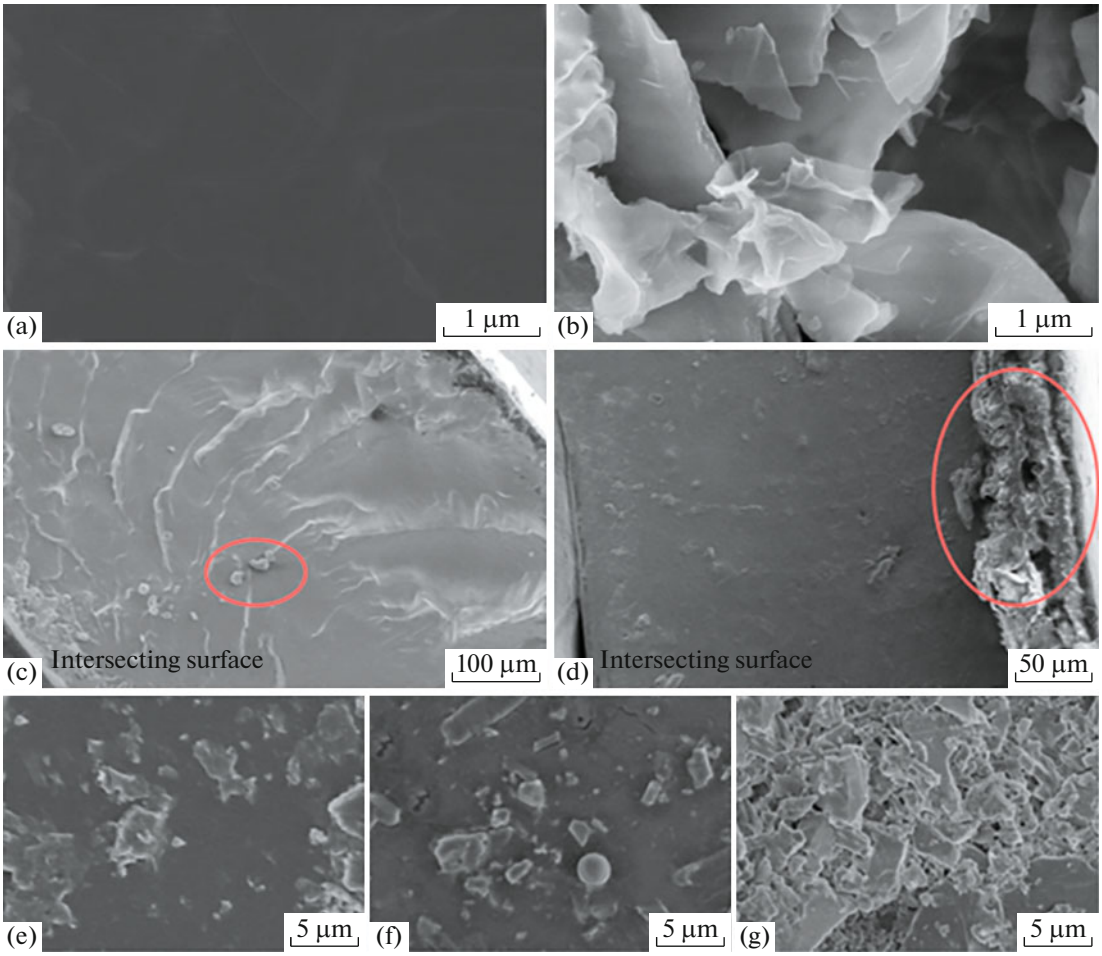

Fig. 5. SEM images of (a) GO, (b) f-GO, (c) f-GO/WPU composite cross-section, (d) GO/WPU composite cross-section; (e) f-GO/WPU composite surface, (f) GO/WPU composite surface center section; (g) GO/WPU composite surface edge section.

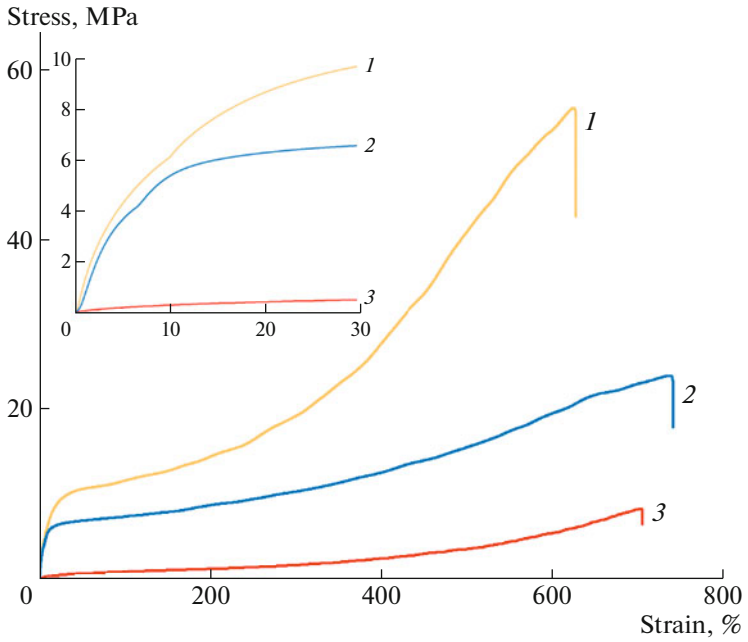

Fig. 6. Stress-strain curves for (*1*) f-GO/WPU composites, (*2*) GO/WPU, and (*3*) WPU.

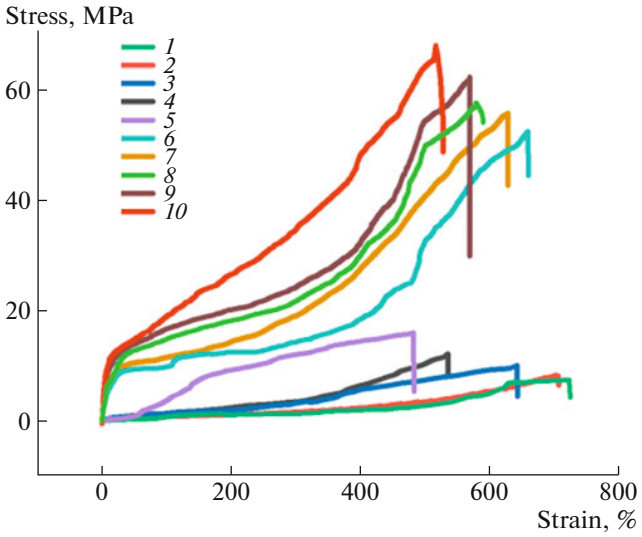

Fig. 7. Stress-strain curves of composites with different GO contents: (*1*) 0.2, (*2*) 0.5, (*3*) 1, (*4*) 2, (*5*) 4% and f-GO contents: (*6*) 0.2, (*7*) 0.5, (*8*) 1, (*9*) 2, (*10*) 4%.

Figure 9 shows the TGA curves for the f-GO/WPU composites, GO/WPU and WPU materials. All three curves show a small mass loss until the temperature is increased to 100°C. This mass loss is mainly attributed to the small amount of water molecules adsorbed on the sample. f-GO/WPU composites started decomposition at 268°C, i.e. higher than that of WPU. For f-GO/WPU composites, the temperature at the maximum thermal decomposition rate is 400°C with a weight loss of 86.5%. The temperature at the maximum rate of thermal decomposition of WPU is lower at 396°C with a weight loss of 82.9% and the lowest for GO/WPU composites by physical mixing was 320°C with a weight loss of 69.7%. The thermal decomposition temperature at 5% weight loss was a highest 213°C when it came to the f-GO/WPU composite, 177°C for the pure WPU and 89°C for the physically blended GO/WPU material. The thermal decomposition temperature ranking did not change for the three samples at 10% weight loss, with T10% of 263, 247, and 140°C for f-GO/WPU, WPU and GO/WPU respectively. Overall, the thermal stability ranking was f-GO/WPU > WPU > GO/WPU. The excellent thermal stability of f-GO/WPU was mainly derived from the cross-linking of silicon-oxygen groups on the molecular chains of f-GO/WPU [17]. In addition, the average bond energy of Si–O was higher than that of C–O and C–C, resulting in increased thermal stability of the f-GO/WPU composites. The weight loss of the composites can be divided into three main stages. The first stage is 25–260°C, where the weight loss mainly comes from the vaporization of residual moisture in the adhesive film and the loss of oligomers. The second stage is 260–360°C, where the weight loss mainly originates from the decomposition of the hard WPU segments. The third stage is 360–460°C, where the weight loss is caused by the decomposition of residual polyurethane molecular chains and silicone groups [18].

CONCLUSIONS

In this paper, physically mixed GO/WPU composites, f-GO and f-GO/WPU composites were prepared

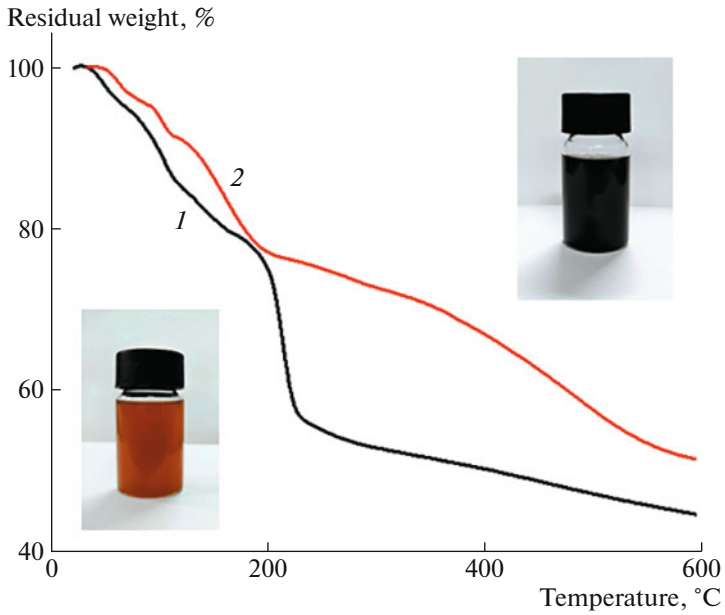

Fig. 8. TGA curves for (*1*) GO and (*2*) f-GO.

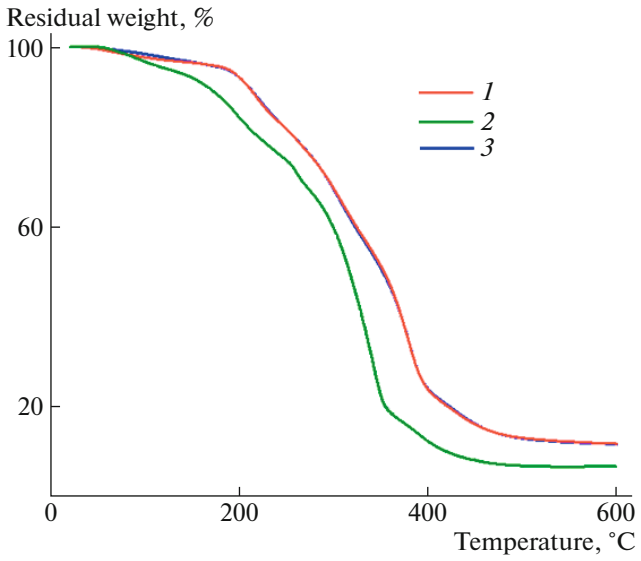

Fig. 9. TGA curves for (*1*) f-GO/WPU composites, (*2*) GO/WPU and (*3*) WPU materials.

and characterized by FTIR and XRD tests. f-GO was proved to be homogeneously dispersed in the WPU matrix by SEM tests, while the physically mixed GO/WPU appeared to have the situation that GO deposited on the polymer surface, which corroborated with the XRD test results. The mechanical tests demonstrated that the introduction of f-GO resulted in an increase in the tensile strength of the composites with a corresponding reduction in elongation at break. The physically mixed GO/WPU mechanical properties were reduced mainly due to the non-uniform GO dispersion. TGA tests showed that the thermal stability of f-GO was superior to that of GO, and the temperature of f-GO/WPU composite was elevated by 16°C at 10% weight loss compared to pure WPU.

Experiments have shown that it is feasible and effective to improve the properties of WPU emulsions by means of composite f-GO. The homogeneously dispersed f-GO/WPU composites can substantially improve the mechanical properties and thermal stability of WPU, solving the problems of poor thermal stability and mechanical properties of water-based inks.

FUNDING

The authors acknowledge the usage of SEM, TEM, FTIR and XPS supported by the Open Subsidies for large-scale Equipment of Wuhan University (Grant no. LF20201282). It was funded by the National Natural Science Foundation of China (Grant no. 51776143), Hubei Provincial Natural Science Foundation of China (Grant no. 2021CFB215) and Wuhan University postgraduate research credit course project of Intelligent Packaging and Food Safety (Grant no. 1506/413100017).

CONFLICT OF INTEREST

The authors declare that they have no conflict of interest.

REFERENCES

1. A. K. Geim and K. S. Novoselov, Nature Mater. **6**, 3 (2007).
2. K. S. Novoselov, A. K. Geim, and S. V. Morozov, Science **306**, 5696 (2004).
3. G. Kaur, R. Adhikari, and P. Cass, RSC Adv. **5**, 120 (2015).
4. Y. J. Kim and B. K. Kim, Colloid Polym. Sci. **292**, 1 (2014).
5. T. Wan and D. Chen, Prog. Org. Coat. **121**, 73 (2018)
6. X. Zhu, W. Zhang, and G. Lu, ACS Nano **10**, 21 (2022)
7. M. B. Kale, Z. Luo, X. Zhang, Polymer **170**, 43 (2019)
8. L. Lei, Y. H. Zhang, and C. B. Ou, Prog. Org. Coat. **92**, 85 (2016)
9. C. Xiang, *PhD Thesis*, Guangdong, South China Univ. Technol., 2020.
10. Y. J. Ma and L. J. Zhi, Acta Phys.-Chim. Sin. **38**, 1 (2022).
11. S. Stankovich, D. A. Dikin, and R. D. Piner, Carbon **45**, 7 (2007).
12. X. Wang, W. Y. Xing, and L. Song, Surf. Coat. Technol. **206**, 23 (2012).
13. Y. G. Zhuo, *PhD Thesis*, Hebei, Yanshan Univ., 2018.
14. L. Liang, *PhD Thesis*, Guangdong, South China Univ. Technol., 2015.
15. X. Y. Qi, K. Y. Pu, and X. Z. Zhou, Small **6**, 5 (2010).
16. J. P. Rourke, P. A. Pandey, and J. J. Moore, Angew. Chem. Int. Ed. **50**, 14 (2011).
17. S. K. Gaddam, S. N. R. Kutcherlapati, and A. Palanisamy, ACS Sust. Chem. Eng. **5**, 8 (2017).
18. L. H. Zhang, Z. H. Zhang, and J. S. Guo, Ind. Eng. Chem. Res. **51**, 25 (2012).